A Visual Analytics Approach for Ecosystem Dynamics based on Empirical Dynamic Modeling

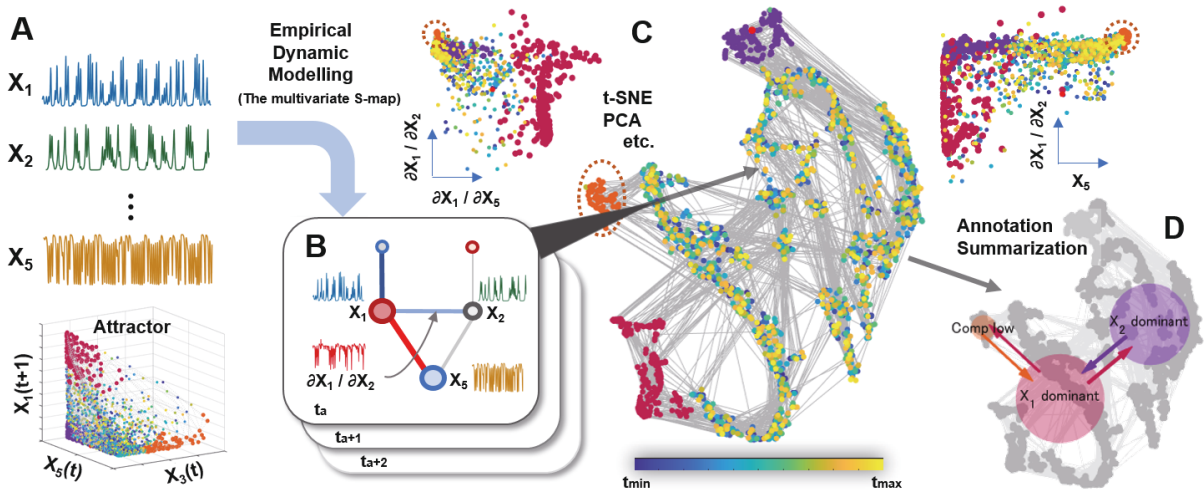Hiroaki Natsukawa, Ethan R. Deyle, Gerald M. Pao, Koji Koyamada, and George Sugihara

Fig. 1. Schematic of visual analytics to study nonlinear interactions with empirical dynamic modeling (EDM). A dynamic graph of changing interaction coefficients is first constructed using the (A) measured time series data and (B) interaction coefficients extracted via EDM techniques. (C) Our proposed visual analytics system enables the detection and interpretation of system states using dimension reduction and brush-link visualization techniques. (D) Using the process of annotation and summarization, the state transition graph can be obtained for interpretation.

Abstract—An important approach for scientific inquiry across many disciplines involves using observational time series data to understand the relationships between key variables to gain mechanistic insights into the underlying rules that govern the given system. In real systems, such as those found in ecology, the relationships between time series variables are generally not static; instead, these relationships are dynamical and change in a nonlinear or state-dependent manner. To further understand such systems, we investigate integrating methods that appropriately characterize these dynamics (i.e., methods that measure interactions as they change with time-varying system states) with visualization techniques that can help analyze the behavior of the system. Here, we focus on empirical dynamic modeling (EDM) as a state-of-the-art method that specifically identifies causal variables and measures changing state-dependent relationships between time series variables. Instead of using approaches centered on parametric equations, EDM is an equation-free approach that studies systems based on their dynamic attractors. We propose a visual analytics system to support the identification and mechanistic interpretation of system states using an EDM-constructed dynamic graph. This work, as detailed in four analysis tasks and demonstrated with a GUI, provides a novel synthesis of EDM and visualization techniques such as brush-link visualization and visual summarization to interpret dynamic graphs representing ecosystem dynamics. We applied our proposed system to ecological simulation data and real data from a marine mesocosm study as two key use cases. Our case studies show that our visual analytics tools support the identification and interpretation of the system state by the user, and enable us to discover both confirmatory and new findings in ecosystem dynamics. Overall, we demonstrated that our system can facilitate an understanding of how systems function beyond the intuitive analysis of high-dimensional information based on specific domain knowledge.

Index Terms—Visual analytics, empirical dynamic modeling, dynamic network, exploratory data analysis

✦

1 INTRODUCTION

• *Hiroaki Natsukawa and Koji Koyamada are with Kyoto University. E-mail: {natsukawa.hiroaki.3u, koyamada.koji.3w}@kyoto-u.ac.jp.*
• *Ethan R. Deyle is with Boston University. E-mail: edeyle@bu.edu. This work was started when he was with Scripps Institution of Oceanography, University of California, San Diego.*
• *Gerald M. Pao is with Salk Institution for Biological Sciences. E-mail: pao@salk.edu.*
• *George Sugihara is with Scripps Institution of Oceanography, University of California, San Diego. E-mail: gsugihara@ucsd.edu.*

Natural systems are often complex and dynamic; therefore, relationships between measured time series variables are generally not static; instead, these relations dynamically change in either a nonlinear or state-dependent manner. For example, in ecology, competition between small desert mammals changes with the amount of rainfall [25,26]; or predation on insect herbivores varies with vegetation structure [19]. To achieve sustainable use of marine resources and conservation of ecosystems, such as those listed in the sustainable development goals (SDGs) [48], it is necessary to monitor the abundance of species included in the ecosystem and understand the interspecies relationship, which changes depending on the state of the system. Moreover, we must understand what type of state the ecosystem has and how this state changes over time.

Because it is difficult to accurately quantify these time-varying interspecies relationships using a conventional linear approach, Deyle et

al. proposed a state-of-the-art method that specifically measures relationships changing in a state dependent manner between time series variables; this method is one element of empirical dynamic modeling (EDM) [15]. EDM is a collection of methods to study systems using attractors reconstructed from time series data based on nonlinear state space reconstruction. Specifically, this is an equation-free approach with minimal assumptions for inductive data-science explorations of natural complex systems. In the function of EDM, time-varying interactions can be calculated using the measured time series data, with this information defining a dynamic network. Therefore, assuming that the measured time series data constitute a node, and each relationship of the nodes constitutes an edge, we can construct a time-varying graph in which the nodes and edges change over time. A time-varying graph representing an ecosystem can provide us with a deeper understanding of the ecosystem; EDM has been used in recent ecological research [15,49–51].

A core strength of data-driven nonlinear analysis, such as EDM, is that system dynamics are not prescribed a priori, but inferred from empirical evidence. A fundamental weakness can be the overwhelming task of interpreting results and identifying intersystem drivers. This involves examining not only the individual relationships between species but also the environmental factors under which relationships are observed. It can also involve interpreting the system state that encompasses the interspecies relationships and examining its shifts such as a regime shift that is large, persistent changes in the structure in ecology. Furthermore, because the relationships between the factors analyzed often occur in four or more dimensions, it is impossible for most people to intuitively understand the results. For these reasons, visualization tools are essential for domain scientists to understand the complex state-dependent relationships between variables, i.e., time-varying graphs. Therefore, in order to overcome the weaknesses of EDM that may require these tasks and to better understand dynamic systems, we investigate integrating methods that appropriately characterize these dynamics (i.e., EDM) with visualization techniques that can help analyze the behavior of the system.

Thus, as illustrated in Figure 1, we developed a visual analytics system that links the construction of dynamic networks, state identification, annotation, and the construction of a state transition graph (STG) by summarizing 2D trajectories. The proposed system supports the identification and interpretation of the system state using EDM-constructed dynamic graphs. In closer collaboration with researchers in the ecology domain, analysis tasks have been summarized and listed for the system design. To demonstrate the usefulness of our proposed system, we applied our proposed system to ecological simulation data and real marine mesocosm data as two distinct use cases, and discovered both confirmatory and new findings in ecosystem dynamics.

Overall, the primary contributions of our study are as follows:

- Defining analysis tasks for a visual analysis system to understand ecosystem dynamics.

- Developing a visualization system that integrates EDM with a visual analytics approach.

- Demonstrating the usefulness of our approach using ecological real-world and synthetic datasets with case studies.

2 RELATED WORK

Dynamic Graph Visualization: With the increased availability of time series data, dynamic graph visualization has been adapted for in several application areas. Two well-known conventional methods for visualizing static graphs are node-link diagrams and adjacency matrices; there are several methods for handling this time dimension because dynamic networks depict a dimension of time, as discussed previously [6,9,47]. Animation and small-multiple methods are examples of time-to-time and time-to-point approaches, respectively. The use of animation to capture network changes can prove to be difficult because of a high cognitive load [5], while the use of small-multiples is associated with the problem of maintaining a suitable level of information

due to space limitations. Therefore, to investigate the global features of a given graph structure and the properties of its edges and nodes in detail, it is important to combine these approaches and/or adopt additional techniques such as linked views and incorporating user interactions. In [6], Beck et al. provided a detailed survey of dynamic graph visualization.

Visual Analytics for Dynamic Graphs: Interactive and linked views not only enable users to filter the dynamic network in various manners but also enable users to reduce the data to a manageable size. Numerous visual analytics systems for exploring dynamic networks have been proposed. For example, Von Landesberger et al. proposed a visual analytics tool to analyze and compare contagion networks using a dimension reduction method [56]. Further, to analyze temporal patterns in dynamic graphs, Burch et al. proposed a matrix-based visualization [12], whereas Hadlak et al. proposed a brush-link visualization with node-link diagrams and time series plots [20].

Steiger et al. proposed analytics that evaluate similarities between time series data obtained from sensor networks using the dimension reduction method [39]. In addition, there are other visual analytics methods for dynamic networks that approach such networks from the viewpoint of degrees of interest [1] and community detection [17]. Although these methods are effective in their respective contexts, it is difficult to specify the state of the given system (e.g., identifying stable, recurring, and outlier states).

Van den Elzen et al. proposed a visual analytics system for dynamic networks using a snapshot-to-point approach [52]. This method represents information on the edges of a dynamic network as a high-dimensional point, and maps these points into two dimensions using a dimension reduction method; note that this method further identifies the system state using a two-dimensional scatterplot. Using this method also enables us to identify stable, recurring, outlier, and transition states; therefore, this method is useful in understanding the structural features of a dynamic network. As reported in the survey paper [11, 31], the main tasks related to visualizing dimensionality reduction results include identifying the clusters in the dimensionality reduction results and understanding the characteristics of the clusters. Furthermore, since the snapshot-to-point method traces the trajectory, another task is to examine the transitions between the identified clusters.

State-Transition Graphs: Visual analytics approaches for meta-networks (i.e., state-transition graphs) of specified system states exist [4, 35, 55]. Adrienko et al. proposed a semantic analysis method of movement behaviors using a state-transition graph that supports comparison between data subsets [4]. In a part of our interpretation process, similar to Adrienko's proposal, an STG is constructed as a meta-network to promote semantic analysis of ecosystem dynamics.

As shown in this brief review, there are various visualization and interaction techniques to support the phenomenological analysis of dynamic graphs. Here, we do not aim to propose another technique. What distinguishes it from the other methods for analyzing dynamic graphs is the explicit reference to an underlying attractor, and in particular the requirement that the multivariate subspace representation is valid, i.e., that the embedding has valid coordinates (we use forecasting to validate). Our goal is to propose a visual analytics workflow by combining EDM with visual analytics approaches including snapshot-to-point and visual summarization using STG to gain new insights into real-world systems.

EDM Resources: Finally, the method to track relative changes between time series variables (one element of EDM) was developed by Deyle et al. [15], and the corresponding code implemented in the R package (rEDM) [44] and python library (pyEDM) [45] are provided. Convergent cross mapping (CCM) [42,58] is a causal inference method using state space reconstruction, which is another element of EDM. The original library of CCM is provided as part of the R package [42]. In addition, studies have proposed other tools in other languages that extend the application of CCM [28]. Furthermore, in [30], we reported our visual analytics approach for supporting the CCM analysis process; however, there is no visual analytics tool available to support the identification and interpretation of the system state based
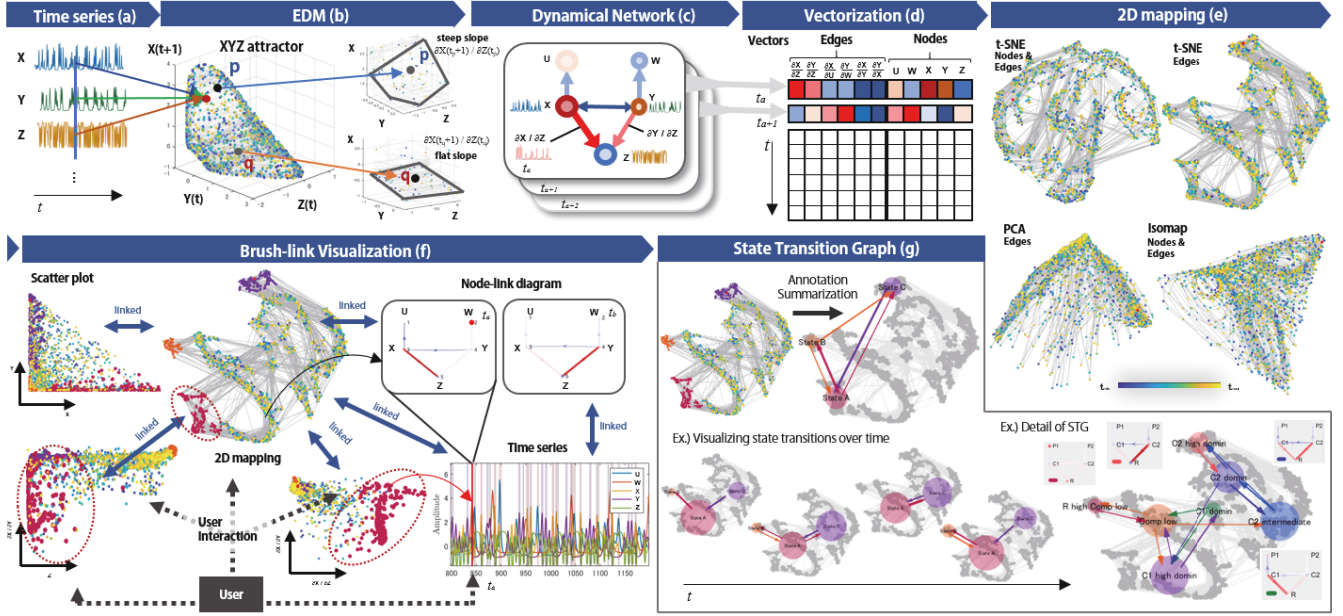
Fig. 2. Workflow of our visual analytics approach. Visual analytics applied to changing interactions with EDM consists of the following steps: (a) preparation of the time series data; (b) empirical dynamic modeling; (c) construction of the dynamic network; (d) vectorization; (e) two-dimensional mapping; (f) brush-link visualization; and (g) annotation and construction of a state transition graph.

on EDM. Therefore, integrating the appropriate visualization technology with EDM can contribute to the analysis in not only ecology but also various other fields.

3 EMPIRICAL DYNAMIC MODELING (EDM)

In this section, we briefly describe the principles and theoretical background of EDM. EDM is an equation-free mechanistic modeling approach based on the principle of reconstructing the underlying dynamic system from an observed time series [14, 16, 40–43]. EDM enables several applications, including being able to determine the complexity of a system, determine the causal variables, and track the strength and sign of each interaction [13]. In this study, we use EDM to track time-varying interactions. As described in the short one-minute video animation (https://youtu.be/fevurdpiRYg), the state of a dynamic system represents a specific location in a multivariate state space whose coordinate axes are causally coupled variables such as fish abundance, salinity, temperature, or resources in ecology. Here, the system state varies in time according to equations that describe system dynamics, tracing out a trajectory. The collection of these trajectories configures a geometric object referred to as an attractor manifold, which empirically describes how variables are related to one another in time. Thus, the attractor is reconstructed from time series data using a multivariate embedding.

The fundamental capability of EDM is the ability to recalculate a partial derivative at each successive state along the attractor [43]. This hitherto unrealized ability allows tracking states on an attractor in order to study how variables in nature interact and change with respect to each other. These partial derivatives are calculated by the multivariate S-map, which is a locally weighted multivariate linear regression method [15, 43] that approximates the best local linear model by providing greater weight to neighborhood points on the attractor that are near the current system state (see Supplementary material for details). S-map iterates this computation at each point of the multivariate attractor and calculates a local linear model C at each time point on the attractor. The coefficients of the local linear model C represent the interaction strength between variables. Here, "interaction strength" is defined as a partial derivative in a multivariate state space, quantifying the interactions between two variables.

In Figure 2(a), we present a schematic of a hypothetical system consisting of three variables in a food web model [21, 34]. The empirical

attractor manifold for this system is constructed using the given time series, as illustrated in Figure 2(b), by taking the three time-series variables as Cartesian coordinates, $s(t) = \{X(t), Y(t), Z(t)\}$ and plotting the system trajectory.

Here, we can observe that the two points on the hypothetical attractor, i.e., points p and q, represent specific states, as illustrated in Figure 2(b). Zooming in on the small neighborhoods of these two points shows that the interactions between X and the other variables are almost linear. The surface at p has a steep positive slope in the Z direction, indicating a positive dependence on Z. Conversely, the surface at q has a flat slope in the Z direction, indicating X is not sensitive to changes in Z at point q. Therefore, the partial derivatives $\partial X / \partial Z$ corresponding to these slopes define the interaction strengths for the system states at points p and q and show the state dependency. These interaction strengths are quantified along its attractor by the multivariate S-map.

Essentially, EDM is an approach that encompasses the various elements mentioned above; however, we use the term EDM as a specific application for calculating time-varying interactions hereafter.

4 VISUAL ANALYTICS APPROACH

In this section, we describe our visual analytics approach. First, we list the analysis tasks for system design. Next, after detailing the application of EDM and listing the necessary data inputs, we describe the dynamic network defined using the results of EDM. Finally, we explain some specific steps behind this approach, i.e., network modeling and vectorization (Section 4.3), dimension reduction (Section 4.4), and visualization and user interaction (Section 4.5).

4.1 Analysis Tasks

Our first goal is to list the analysis tasks for achieving the goals of identifying and interpreting the ecosystem dynamics from EDM results. To this end, we discussed with three co-authors (SC1, SC2, SC3) and three scientific collaborators (SC4, SC5, SC6), all of whom were familiar with EDM, nonlinear dynamics and oceanography. SC1-4 were domain scientists, and SC5-6 were graduate students in oceanography. To date, the core results published utilizing EDM have generally results describing what kind of interaction between species and under what conditions through basic visualizations such as scatterplots. This is a very sound approach for doing environmental data science, but
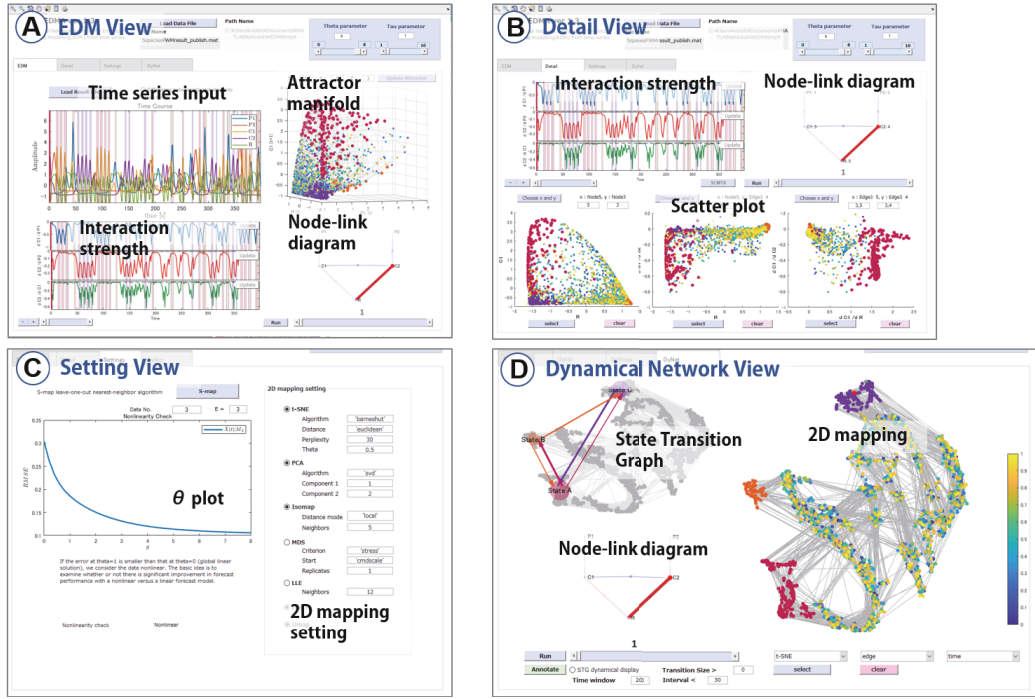
Fig. 3. Graphical user interface (GUI) screenshots of our proposed visual analytics system. GUI of our prototype consists of four tabs of views: (a) EDM view enabling confirmation of the input and output of EDM; (b) detail view with multiple scatterplots enabling exploration of the relationships between the variables; (c) setting view supporting the determination of the value of θ; and (d) dynamic network view with dynamic graph, two-dimensional mapping, and state transition graph for identification and interpretation of the system state.

also does not address the potential for visual analytics to also be hypotheses generating. The tasks for understanding the global and local features of the results also were not organized, and no graphical user interface (GUI) or visual analytics approach to support EDM analysis has been available to date. To address these issues, we proposed a visual analytics system combining EDM and visualization techniques to tackle these challenges. After multiple rounds of discussion, we derived the following four analysis tasks (**AT**) that our system should provide.

AT1 : Confirming EDM results including the relationship between the variables and sign of the interaction.

AT2 : Identifying states from EDM-constructed dynamic graph.

AT3 : Understanding and annotating identified states.

AT4 : Visualizing and understanding of transition relationships between states.

We designed the visual analytics system based on these requirements. A workflow of our system is shown in Figure 2. In the next subsections, we explain the workflow in detail.

4.2 Empirical Dynamic Modeling (EDM)

In general, EDM consists of several steps.

First, we calculate a dynamic network using EDM, as illustrated in Figure 2(a) and 2(b). In this step, the interactions between time series data are quantified via EDM, thereby enabling the construction of a dynamic network. As noted above, we assign the measured time series data to nodes of the network and interactions between the time series data to edges of the network, as illustrated in Figure 2(c).

As an example, we used the time series data from the five species food web model with two consumers (X, Y), their predators (U, W), and a single resource (Z), as shown in Figure 2(a) to calculate the interaction strengths among variables based on the ecological relationship. First, the state space is reconstructed using each variable. Let us

suppose we use variables X, Y, and Z for the reconstruction, as illustrated in Figure 2(b). Note that EDM results are sensitive to the choice of variables to be embedded; therefore, in real systems, it is important to causally choose coupled variables to be embedded in advance (see Supplementary material in detail). Normally, variables are chosen using the causal inference method such as CCM [42] as in the case described in a previous study [15] and a recent paper [50]. The variable selection method (i.e., CCM calculation) is not included in the process of our proposed tool; however, our proposed tool calculates EDM using a chosen set of variables by inputting adjacency matrices that define causally coupled relationships.

Second, we determine the optimal weighting parameter θ used in the S-map. θ is a nonlinear parameter that controls how strongly the points near the target in a multidimensional state space are weighted in the regression (see Supplementary material for details). θ must be determined in advance, and a general way to choose an appropriate θ is to examine the prediction error as a function of θ. In our proposed system, the optimal parameter, θ, can be determined by the univariate's S-map [43] calculated in the Setting view in Figure 3(c). If user push the S-map button, the univariate's S-map is automatically calculated; user can confirm the prediction error as a function of θ. We determine θ value that shows the minimum prediction error as an optimal parameter to control local linearity, which can then be used in the corresponding EDM calculations (see Supplementary material for discussion of θ parameter).

Third, partial derivatives $\partial X/\partial Z$, and $\partial X/\partial Y$ etc. are calculated at each point using the multivariate S-map method. The results indicate that the interaction strengths fluctuate in the attractor, as shown in Figure 2(b).

4.3 Dynamic Network Model and its Vectorization

In a previous subsection, $\partial X/\partial Z$ and $\partial X/\partial Y$ were calculated from the time series data of X, Y, and Z via EDM. Assuming the relationships, $[\partial X/\partial Z, \partial Y/\partial Z, \partial X/\partial U, \partial Y/\partial W, \partial X/\partial Y, and \partial Y/\partial X]$, are calculated in the same manner as shown in Figure 2(c), a dynamic network Γ can be modeled as a sequence of N snapshots, i.e.,

$$\Gamma = (G_1, G_2, \cdots, G_N), \qquad (1)$$

where snapshot G_i is the directed graph $G_i = (V_i, E_i, t_i)$ with node (vertex) set V_i, edge (link) set E_i, and t_i denoting the i-th time step. Let the weights of the edge and node be v_i and e_i, respectively. Subsequently, v_i and e_i can be defined as $v_i = [U(t_i), W(t_i), X(t_i), Y(t_i), Z(t_i)]$ and $e_i = [\partial X(t_i+1)/\partial Z(t_i), \partial Y(t_i+1)/\partial Z(t_i), \cdots, \partial Y(t_i+1)/\partial X(t_i)]$. In the dynamic network graph, $\partial X/\partial Y$ is represented as the directed edge from X to Y. Conversely, $\partial Y/\partial X$ (i.e., the influence of X on Y) is represented as the directed edge from Y to X.

In the next step, snapshots of the constructed dynamic network are vectorized as shown in Figure 2(d). Because each snapshot contains information regarding edges and nodes at a particular time point, G_i can be represented as matrix M_i of size $1 \times (|V| + |E|)$, where $|V|$ and $|E|$ denote the number of nodes and edges, respectively. We therefore obtain a series of N matrices with snapshots that can be used together to define the dynamic network. These snapshots are then interpreted as a point in a high-dimensional space. To analyze the dynamic network, we used the snapshot-to-point approach. Here, all N network snapshots represent an $N \times (|V| + |E|)$ matrix, as depicted in Figure 2(d). Specifically, columns of this matrix represent the nodes and edges of the network, and rows represent different snapshots.

4.4 Dimension Reduction Process

Because multiple dimensions are difficult to grasp and visualize, our next step is to reduce and project high-dimensional points onto the more manageable two dimensions using dimension reduction algorithms [54], as illustrated in Figure 2(e). Numerous linear and nonlinear dimension reduction algorithms are available, including principal component analysis (PCA) [22, 32], muti-dimensional scaling (MDS) [24], Isomap [46], locally linear embedding (LLE) [37], and t-distributed stochastic neighbor embedding (t-SNE) [27]. As implementation of t-SNE, we decided to use the Barnes-Hut-SNE technique [53] to reduce the computation times of the t-SNE approach. A comparative survey of dimension reduction algorithms helped us conclude that nonlinear algorithms perform well on selected artificial tasks [54]; however, PCA is still used on many real-world datasets and easy to interpret. Therefore, we adopted the above five algorithms to encourage users to select an algorithm that is best-suited to their specific study, as illustrated in Figure 5.

Finally, as shown in Figure 2(e), high-dimensional information regarding a dynamic network is visualized in a two-dimensional space. In two-dimensional mapping, a node represents a snapshot at a certain time point in the dynamic graph, and nodes at adjacent time points are connected by links. The position of the resulting two-dimensional mapping provides insight into the evolution of the network. We can evaluate the similarity between snapshots of a dynamic network, thereby identifying and characterizing various states of the network. The goal to use a dimension reduction plot is the identification of system states that is represented by a cluster of similar network "snapshots".

4.5 Visualization and Interaction

For the final step, we introduce a visual analysis system that includes brush-link visualizations [23], annotation of identified states, and visual summarization of state transition information as an STG.

To explore a dynamic network based on EDM, we developed a GUI with multiple views as a prototype of the application. Our system is implemented in MATLAB, which is a programming environment for numerical and technical applications. We used MATLAB GUIDE (GUI development environment) to create all UIs. EDM, dimension reduction calculation, plots, user interactions, and animations were implemented using the built-in functions and toolboxes of MATLAB. Figure 3 shows screenshots of our developed GUI, which contains four tabs: EDM view, detail view, setting view, and dynamic network view. In general, standard interactions such as zooming, rotation, and data cursor, are available in all views. The plots shown in each view are created by loading data from the upper load button.
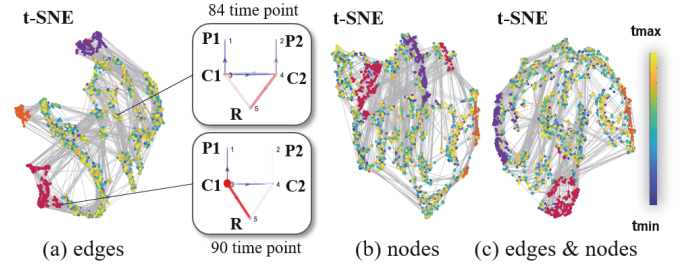

Fig. 4. Selection of the dataset. Users can specify the dataset used to generate the two-dimensional mapping plot. The pop-up menu enables users to select datasets with (a) all edges, (b) all nodes, or (c) all edges and nodes. The selected dataset is vectorized and used for two-dimensional mapping. Two-dimensional maps applied to the five-species food web dataset with the above data selections are plotted here. The point group selected by user interaction are highlighted. The color of the points represents the time point using the multihued sequential colormap.

EDM View   For the EDM view (i.e., Figure 3(a)), users can confirm the input time series, calculated interaction strength, the attractor, and a snapshot of the dynamic network (i.e., node-link diagram), supporting **AT1**. The upper left plot in Figure 3(a) shows the input time series data; the plot on the upper right is the attractor plot with a multivariate embedding, which can be used to understand the relationship between the variables. The color of the attractor plot represents the sampling time point using the sequential color encoding with the multihued scheme, including Blue-to-Green-to-Yellow as shown in the rightmost color bar in Figure 3(d). Blue and yellow color in this colormap indicate the first and the last time point, respectively. Further, the attractor plot is drawn in three dimensions; the attractor is displayed using three user-selected variables. Note that even if the input data have more than four dimensions, they will be displayed with only the three selected variables.

The lower left plots show the time series of the calculated interaction strength. The time series of the interaction strength to be displayed can be changed using the update button shown in the inset in the upper right portion of the plot. The node-link diagram at the lower right is a snapshot of the dynamic network at a specific time, with the color of the nodes and links representing the sign of the time series data, i.e., red corresponds to positive, whereas blue represents negative, supporting **AT1**. Further, the width of the link and the size of the node represent the interaction strength and the amplitudes of the time series data, respectively. When the "Run" button located next to the plot is pushed, the animation is displayed, with the slider available to update the snapshot at any arbitrary time. Note that we adopted animation to show the snapshot considering the space efficiency of the GUI. The time of the snapshot is represented with a red vertical line in other time series plots, and the state of the corresponding time is highlighted in red in the attractor plot (Supplementary Figure SF1). In the animated display, the corresponding time is incremented automatically.

Detail View   In the detail view (i.e., Figure 3(b)), in addition to the interaction strength and snapshot of the dynamic network displayed in the EDM view, a scatter diagram depicting the relationship between the user selected nodes and links is visualized. This view enables users to explore the relationships between nodes and links in which the user is interested, supporting **AT1-3**. The three bottom figures of Figure 3(b) are scatterplots showing the relationship between the nodes and links. Once the user designates the node number or link number (e.g., a user can specify the link from node 3 to node 1 by typing "[3, 1]" in the editor), the scatter diagram between the specified nodes and edges can be plotted. The color of the scatterplot represents the time point with the same color encoding as that in the attractor plot.

Setting View   In the setting view (i.e., Figure 3(c)), the prediction error as a function of θ for the univariate embedding of selected vari-
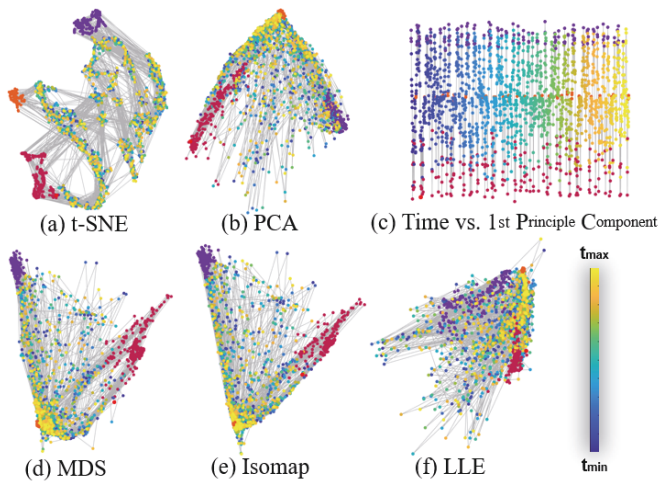
Fig. 5. Linear and non-linear dimension reduction methods. Dimension reduction methods (a) t-SNE, (b) PCA, (c) time vs. first principal component, (d) MDS, (e) Isomap, and (f) LLE applied to the five-species food web dataset in our first use case study are illustrated. Note that t-SNE separated the states, whereas the other methods except for (c) summarize the features of the dynamical network in a similar way.

ables is plotted. From this result, users can specify a θ value to use for EDM. In this view, users can confirm the prediction performance with respect to θ and can determine θ with the best prediction in the S-map. In the setting view, the user can also specify parameters to use for two-dimensional mapping (e.g., perplexity in t-SNE, number of nearest neighbors in LLE and Isomap).

Dynamic Network View   In the dynamic network view (i.e., Figure 3(d)), users can observe and interact with the two-dimensional mapped scatterplot of the dynamic network, a snapshot of this network, and a state transition graph constructed by identifying the states. Specifically, this view enables users to explore and identify the system state using two-dimensional projection mapping, supporting **AT2-4**. In the 2D mapping scatterplot, the color of the plot represents the time point with the same color encoding as that in the attractor plot. Because the nearby points in time on the scatterplot are connected by edges, it is possible for users to grasp the dynamics of changing system states.

The users can also select a specific dimension reduction algorithm, introduced in Section 4.4, using the pop-up menu beneath the plot. When points are repositioned because of switching between different projections, the user's mental map is preserved through animation. In addition to selecting a dimension reduction algorithm, users can also specify the dataset used to generate the two-dimensional mapping plot, as shown in Figure 4. In Section 4.3, we noted that all nodes and edges combine to form a point in a high-dimensional space; however, when the users are only interested in nodes or edges, the rightmost pop-up menu enables them to select the dataset they intend to use (i.e., dataset with nodes, edges, or both).

Next, we describe brush-link visualization, annotation of the identified states, and visual summarization of STGs. The brush-link visualization uses two-dimensional projections, scatterplots among variables, time series plot, and node-link diagrams, as depicted in Figure 2(f).

First, users can select point groups on either the scatter diagram of the detail view or the two-dimensional map of the dynamic network view using the lasso selection. The selected point group is then highlighted, and the corresponding data points are highlighted in the other scatterplots. As to time series plot, the time information of the selected point group is linked by highlighting the background area of the corresponding time in the same color. Note that the highlighted color of the selected point group is randomly determined. Further, any of these selections can be deselected using the cancel button beneath the

scatter diagram. By implementing this form of interaction, the users can select the state of the system and visually examine the features of the selected point from the linked plots, supporting **AT2, 3**. If there is a specific feature in the value of nodes or edges in dynamic graphs, it is expected to be visually detected as a separable state on a two-dimensional mapping plot.

Next, as shown in Figure 2(g), we carry out the annotation and summarization steps using the results of brushing and linking. Once a point group is selected by the lasso selection, the node in the STG that aggregates the selected point group is represented as shown in the upper left diagram of Figure 3(d). The STG node is placed at the centroid of the selected point group. Then, the transition between the states in the time window $T = [t_0, t_{last}]$ is acquired as a time-referenced state sequence. Here, t_0 and t_{last} are the earliest and latest time points in the dataset. It is possible to construct an STG not from the entire sequences but from the user-selected time interval $[t_1, t_2]$, $t_1 \geq t_0$ and $t_2 \leq t_{last}$. A directed edge is given between STG nodes based on the calculated number of transitions. The size of the node and the width of the link on STGs represent the number of selected points and transitions between states, respectively. These representations of the STGs support **AT4**. Furthermore, if users want to examine the changes in STGs, a STG is constructed for each interval by a sliding-window, resulting in time-varying STGs (i.e., dynamic STGs). To view the dynamic STGs, users can use the time slider that is used for updating the snapshot of a dynamic graph, supporting **AT4**. Moreover, after analysis of identified states, users can annotate those states semantically, as shown in Figure 1(d), supporting **AT3**. The annotation of the states is represented as a label of the node in STGs.

This tool allows users to move back and forth between these views and visually analyze the dynamic graphs constructed by EDM.

5   USE CASE

To demonstrate the performance of our system, we applied our approach to both artificial and real-world datasets with SC1 and SC2. In the first use case, we describe how EDM functions, and how to use our system to support the interpretation of ecosystem dynamics using an artificial dataset. Then, we presented the results and discussed the choices for settings. Finally, we conducted second case studies with marine mesocosm data and showed how to reach the mechanistic interpretation of ecosystem dynamics by identification, annotation, and visual summarization. Because these datasets have already been analyzed in a previous study [15] without the use of visual analytics tools, we could compare results with previous knowledge in the subsections below.

5.1   Ecological Simulation Dataset

We started our comparison using artificial ecological datasets to test and evaluate our visual analytics approach. The model shown in Figure 6(a) is based on a classic food web topology [21, 34] with two consumers ($C1$, $C2$), their predators ($P1$, $P2$), and a single resource (R). In this particular model, saturating Holling Type II feeding responses, which assume that the consumer is limited by its capacity to process food, govern the species interactions in a food web [15], which gives rise to state-dependent competition [2, 3]. This model simulates the time series data of species abundance. For this demonstration, we focus on measuring the varying effects of ecosystem components on the two consumers ($C1$ and $C2$). The dynamic network of the model shown in Figure 6(a) was analyzed using our tool. The number of variables and calculated interaction strengths are five and six (note the distinction between $\partial C1/\partial C2$ and $\partial C2/\partial C1$), respectively, resulting in that total dimension of a snapshot is eleven.

The results are consistent with those reported by Deyle et al. [15]. Although the strengths vary, there is generally a negative interaction between $C1$ and $C2$ (Figure 6(b)) and a positive effect of R on $C1$ (Figure 6(c)). The scatterplot in Figure 6(e) shows that negative interactions $\partial C1/\partial C2$ (i.e., competition) only occur at low- to moderate-food levels, whereas competition tends to be zero at high food concentrations. Note that the small absolute value of $\partial C1/\partial C2$ means less competition. For interactions $\partial C2/\partial C1$, a similar trend is confirmed.
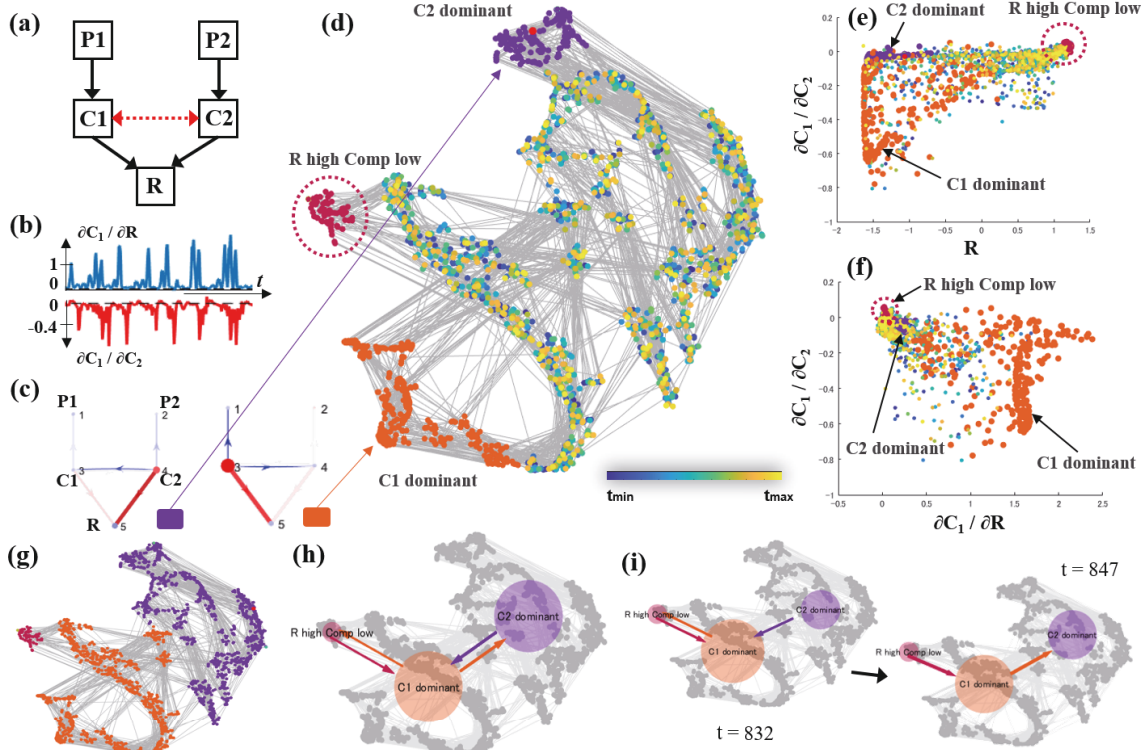
Fig. 6. Results of our ecological simulation use case study. An artificial dataset is simulated as (a) the five-species food web model with interactions between time series data calculated using EDM. (b) The time series plots of calculated interactions ($\partial C1/\partial R$, $\partial C1/\partial C2$) are shown. Here, (c) the resulting dynamical networks are mapped to (d) a two-dimensional space using a dimension reduction method (i.e., t-SNE is used with all edges as the dataset). Next, we show the dependence of the competition on (e) food abundance and (f) food limitation. In (g), three point groups are classified by user interaction. The constructed state transition graph is shown in (h). In (i), the dynamics of STG are shown using a time slider. From the dynamics, we can confirm a typical ecological patterns exhibited by r-strategists ($C1$) and K-strategists ($C2$).

Moreover, $\partial C1/\partial R$ (i.e., a direct measure of food limitations) defines a maximum of the strength of competition (Figure 6(f)).

Next, a 2D mapping view is displayed to identify what type of state is there in the dynamic graph. As shown in Figure 6 (d), separable states were observed using t-SNE algorithms. Figure 6(d) shows those states brushed by user interactions, whereas Figure 6(e) and 6(f) show the placement of selected points in the scatterplots. From these results, one selected point group (highlighted in red) represents states in which R is large and the interspecies competition is small, whereas another selection group (highlighted in orange) characterizes states in which R is small and interspecies competition is large. Consequently, our proposed tool characterizes the features of the system state that matches particular interaction patterns (consistent with results described in the previous work [15]).

Note that even if there is no prior knowledge of ecology, these prominent features can be identified using a dimension reduction mapping using our tool. Figure 5 shows 2D mapping results obtained using various dimensional reduction methods. In this simulation data, t-SNE successfully separates and characterizes the states of the system as described above, whereas the other methods fail to successfully extract these features. Because 2D reduction methods may vary in their effectiveness for different datasets, we cannot draw general conclusions that the t-SNE is superior to the others from these results, but we can conclude that t-SNE fits this type of data. In the next subsection, the results of t-SNE are shown for a use case with real-world data.

Taking a closer look at the 2D mapping view in Figure 6(d), we found a new feature of state (highlighted in purple Figure 6(d)), in which R is small with less competition $\partial C1/\partial C2$, which was not found in the previous research. Other linked scatterplots showed that this state is characterized by large $\partial C2/\partial C1$ (i.e., the effect of $C2$). To develop the state transition graph, we classified the 2D mapping points into three groups including the identified point groups highlighted in

red, purple, and orange, as depicted in Figure 6(g). The constructed state transition graph is shown in Figure 6(h). From the linked scatterplots of the detailed view, as described in the previous subsection, the leftmost group represents the state in which R is large and the interspecies competition is small. Therefore, this group is annotated as "R high Comp low". In contrast, the middle group characterizes the state with larger competition $\partial C1/\partial C2$ (annotated as $C1$ dominant), whereas the rightmost group represents the state with larger competition $\partial C2/\partial C1$ (annotated as $C2$ dominant).

The state transition graph shows that the dominant feature of state transition is the state group change between $C1$ dominance and $C2$ dominance. Interestingly, the $C1$ dominant state is the only state from which we can go to the leftmost states showing abundant R. Once we reach the leftmost state, state transition mainly occurs from the $C1$ dominant state to the $C2$ dominant state. The structure of this 5-species food chain model is identical to that of the equation between two chains; however, different coefficients are set to prevent synchronization between $C1$ and $C2$. The parameters effectively make $C1$ a more r-selected species that can produce many offspring, each of which has a relatively low probability of surviving to adulthood. In contrast, $C2$ becomes a more K-selected species that have longer life expectancies, produce relatively fewer offspring. Because of their higher reproductive rates, primary colonizers are typically r-strategists ($C1$). Eventually, a new equilibrium that may be the leftmost state in the state transition graph is approached, with r-strategists ($C1$) gradually being replaced with K-strategists ($C2$) that are more competitive and better adapted to the environmental characteristics [33]. As shown in Figure 6(i), we can confirm those patterns by a user interaction into the time-varying state transition graph. This use case revealed that the visual analytics approach lead to the characterization of system states and understanding of ecosystem dynamics.
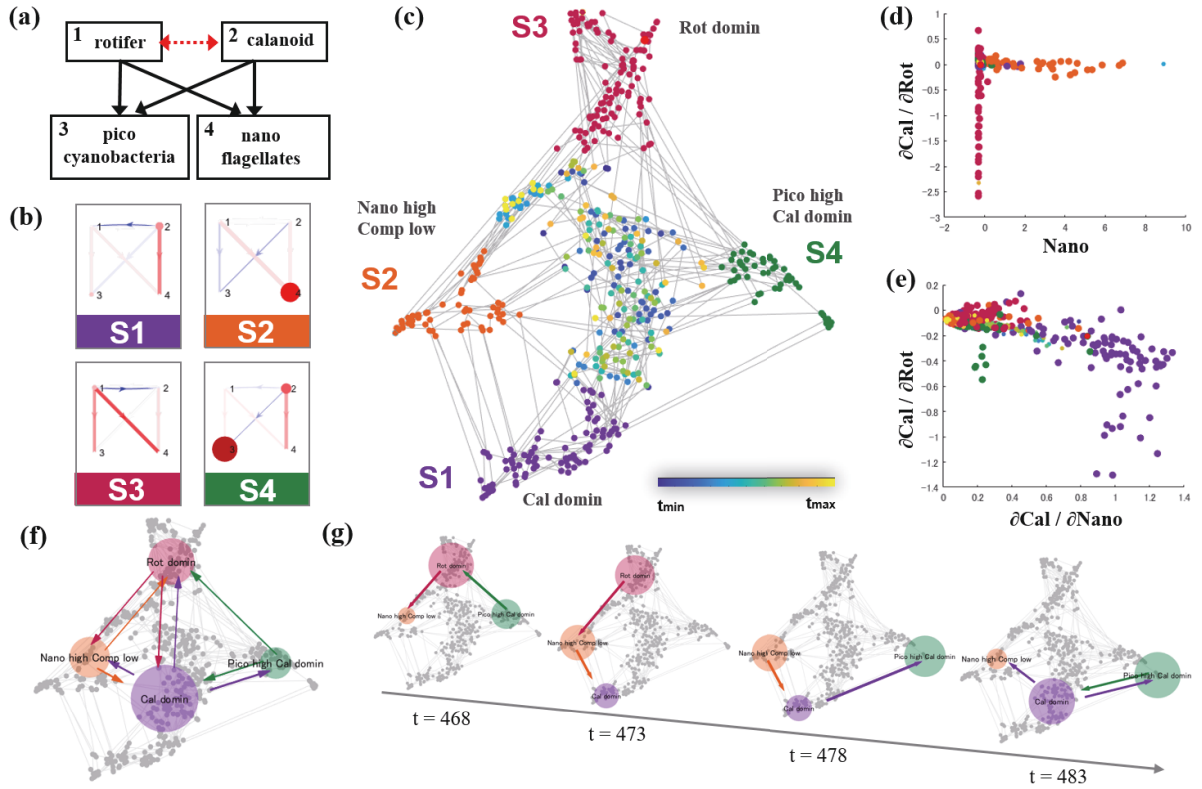
Fig. 7. Results of the use case study for Baltic Sea mesocosm dataset. (a) The focal interspecies food web model in the mesocosm dataset. (b) Four types of system states (S1-S4) are identified by two-dimensional mapping. (c) Dynamic networks with nodes and edges are then mapped to a two-dimensional space using t-SNE. The dependence of competition on (d) food abundance *Nano* and (e) food limitation $\partial Cal / \partial Nano$. (f) 2D mapping points into four groups by user selection and the state transition graph are constructed. Their nodes are annotated as illustrated on the node label. (g) Snapshots of the time-varying state transition graph.

5.2 Mesocosm Experiment Dataset

As the second use case, we applied our proposed method to the marine mesocosm dataset including calanoid copepods and rotifers that are isolated from the Baltic Sea [7,8]. Mesocosm means experimental system that examines the natural environment under controlled conditions. The marine mesocosm data were obtained from the supplemental materials of Beninca et al. [7,8]. Because the sampling interval was not regular, we have interpolated them using spline interpolation to regularize the sampling interval. Similar to our previous study [15], we also focus on calanoids, rotifers, and their two main prey, i.e., nanoflagellates and picocyanobacteria, as modeled in Figure 7(a). Then, we quantified the varying interaction strength to differentiate between the two consumers (calanoids and rotifers) and the other ecosystem components. The number of variables and calculated interaction strengths are four and six, respectively, resulting in that total dimension of a snapshot is ten.

Moreover, the EDM results match those reported by Deyle et al. [15]. Interactions with the chief prey (i.e., nanoflagellates) are always positive, whereas interactions with the other grazer (i.e., rotifers) are always negative. Competition $\partial Cal / \partial Rot$ is strong only when the concentration of nanoflagellates is near zero, as indicated in Figure 7(d).

Further, the user interaction with 2D mapping shown in Figure 7(c) showed several point groups. Figure 7(d) and 7(e) show the placement of the selected points on scatterplots. Figure 7(b) shows how each of these four groupings can be characterized from the scatter diagram, as follows: (S1) states where prey is small and competition $\partial Cal / \partial Rot$ is large; (S2) states where *Nano* is abundant and interspecific competition is small; (S3) states where prey is small with large interspecies competition $\partial Rot / \partial Cal$; and (S4) states where *Pico* is abundant and interspecific competition $\partial Cal / \partial Rot$ is large. Groupings (S3) and (S4) were newly found using our tools. Similar to the

case study for the simulation dataset, the proposed tool enabled us to reconfirm and discover these states efficiently, as well as visually identified these states by 2D mapping without knowledge of the domain.

Because real-world ecosystems are more complicated than the simulation, the possibility that more characteristic states of the system exist than those found in the simulation. In addition, similar to the simulation considerations, we classified the 2D mapping points into four groups including the identified point groups to construct the state transition graph, as shown in Figure 7(f). From the linked scatterplots of the detail view, four groups S1, S2, S3, and S4 are annotated as "*Cal* dominant", "*Nano* high Comp low", "*Rot* dominant", and "*Pico* high *Cal* dominant", respectively, as depicted in Figure 7(f). We can see that the dominant features of the state transition between *Cal* and *Rot*. In contrast to the ecological simulation, both *Cal* dominant state and *Rot* dominant state can transition into the leftmost state showing abundant *Nano*. In addition, competition between *Nano* and *Pico* is observed, in Figure 7(f), because they compete for the same resources. Interestingly, the transition from "*Rot* dominant" to "*Pico* high *Cal* dominant" does not exist in the graph. This is because *Pico* (small phytoplankton) are mainly eaten by *Rot* (small zooplankton), whereas *Nano* (larger phytoplankton) are eaten by *Cal* (larger zooplankton). These size differences can cause an asymmetric transition in terms of *Pico*.

Figure 7(g) visually explains why the system alternates between the two predator-prey cycles. As depicted in the leftmost graph in Figure 7(g), if *Pico* are abundant, the *Rot* population will increase and suppress *Pico*. Therefore, *Nano* can gain a competitive advantage instead of *Pico*, as shown in the second graph. This will benefit *Cal*, which rises in abundance, and subsequently, suppresses *Nano*. This gives new opportunities for *Pico* to seize the available resources, as shown in the third graph. Although this mechanistic explanation was described qualitatively in the discussion section of ref [8], our pro-

posed tool makes it visible through the detection, annotation, and visual summarization of the ecosystem dynamics. Thus, we can reach a mechanistic understanding of the ecosystem dynamics in the marine mesocosm by combining the latest analytics and visual analytics approaches.

6 DOMAIN EXPERT FEEDBACK

We collected feedback from our three experts (SC1, SC2, and SC4) in the fields of oceanography, nonlinear dynamics, and quantitative biology, who are familiar with EDM analysis. They feel that the proposed visual analysis system is a useful tool to interpret ecosystem dynamics based on EDM. SC4 commented, "The GUI is well-designed and intuitive for the researcher familiar with EDM, state space analysis, and nonlinear dynamical systems. The identified workflow is sensible, guiding the user through a multistage analysis regime." SC4 continued, "This work, as detailed in four **ATs** and demonstrated with a GUI, provides a novel synthesis of tools and methods to disentangle seemingly insurmountable state space representations. It thereby constitutes an advancement in the application of nonlinear dynamical analysis." SC2 mentioned that "Since a priori one cannot possibly know what the structure of the data is, the proposed system offers a good selection of dimensionality reduction projections that span a good variety emphasizing both global and local features to allow for data exploration without having to a priori know what the underlying structure is." The experts plan to utilize this tool for neuroscience, not only to know under which circumstances relationships between neurons are positive or negative or don't change but also to develop an intuition for the more global picture among the interacting variables. Overall, the experts are satisfied with our visual analysis system and feel that it meets all of their expected requirements.

7 DISCUSSION

Use cases and domain expert feedback demonstrate the effectiveness of the proposed visual analytics system. This section examines the new insights found in the use cases and discusses how the visual or interaction design of the system made these discoveries possible.

In two use cases, the tool revealed new ecosystem state features (a group with lower R and large $\partial C2/\partial C1$ competition in the first use case and a group with (S3), (S4) in the second use case) and new asymmetric transitions between the identified groups. As seen in related works using EDM [15, 49–51], scatter plots and time series plots are often used to interpret the results of EDM, and AT1-3 are viable in principle by examining the relationships between individual variables and interactions in detail. However, there is a limit to the number of distinctive groups that can be found in the scatterplot alone. In this study, integrating the snapshot-to-points approach with the EDM results allowed us to recognize more global features of dynamic graphs and to identify a greater variety of states (satisfying **AT2**). In addition, the features of a specific group can be analyzed and annotated in detail through linked visualization of each plot with each view in our system, guiding the user through a multistage analysis regime represented as " overview first, detail on demand " [38].

As for the transitions between groups, the more time series points, the more snapshots are generated, and it is difficult to understand the direction and amount of transitions only by looking at the trajectory in 2D mapping. Therefore, in this study, we calculated the characteristics of transitions between specific groups and presented them as node-linked directed graphs that are easy to comprehend intuitively, enabling understanding of the asymmetry of the prey-predation structure in the seemingly symmetric food web model. Although our tool supports only fundamental functions for STGs, visual representation of STGs, as proposed in [10, 36], could be improved to make the state sequence more understandable. In order to analyze the global characteristics of these dynamic STGs, snapshot-to-point [52] and other methods to efficiently show the changes in the dynamic graphs [29] may also be useful.

Although there are several possible candidates for the choice of the plot used in each view, such as histograms of variables and color maps, we have tried to use representations that have been used by experts in the past, with a preference for clearer representations. There may be visual representations and interaction designs that would make this AT more efficient, such as advanced plots or direct encoding of features related to a particular group. EDM is important on its own as a method to quantify time-varying nonlinear interactions; however, its possibilities can be dramatically extended by being associated with a well-designed visual analytic approach. Conversely, although this research does not offer sophisticated progress for the visualization technique itself, basic visual analysis such as brush-link and user interactions can fulfill its potential when combined with state-of-the-art technologies of the given domain.

We implemented five algorithms for dimension reduction. Of these five algorithms, t-SNE successfully separated the states, as we showed in Figure 5, but other algorithms may be effective depending on the given data, as shown in the analysis of a high school communication dataset in a related study [52]. As part of our future work, we plan to identify the most appropriate dimension reduction method and the best distance measure. In our use cases, the numbers of nodes and edges of the dynamic network were not large. From the viewpoint of scalability, we should certainly be able to handle larger networks; however, for EDM calculations, we need to determine the variables to be used for multivariate embedding based on the results of causal inference methods such as CCM. Therefore, we assume that EDM is applied to small- or medium-sized networks whose causal relationship is already expected. In this study, the number of dimensions of the snapshot was set to 10 for the first use case and 11 for the second use case. Although our prototype had a limited number of scatter plots, time series plots, and dimensions (i.e., 3) of the attractor plot, this could be dealt with by switching the variables we wanted to visualize. However, when dealing with large graphs, we will need some computational ideas for efficiently drawing large-scale graphs.

Finally, our current system is a prototype, and there are several directions for future work. Techniques supporting a series of analysis and exploration can be improved by incorporating automatic clustering algorithms into a current workflow, as discussed in ref [57], and an additional supporting analysis to understand the cluster's characteristics, as proposed in ref [18]. Furthermore, comparing data under multiple conditions might also be beneficial. This paper has focused on natural systems, ecosystems, etc.; however, nonlinear dynamical systems are ubiquitous. Applications in geophysics, neuroscience, and synthesis with machine learning, and as subsystem networks or controllers for heterogeneous information processing systems, will also benefit.

8 CONCLUSION

In this study, we proposed a visual analytics system that integrated EDM calculations with interactive visual analytics including brush-link visualization and visual summarization not only to construct dynamic graphs but also to support the identification and interpretation of ecosystem dynamics. To demonstrate our proposed system, we applied our approach to both artificial and real-world datasets. Our use case studies showed how visual analytics tools could be used to identify and interpret system states and deepen our knowledge regarding the underlying rules governing such systems. Our visualization study tool facilitates detailed understanding of how ecosystems work that goes beyond a general analysis of high-dimensional information based on domain knowledge. We expect our proposed method will be useful not only in the field of ecology, but also in many other diverse fields.

REFERENCES

[1] J. Abello, S. Hadlak, H. Schumann, and H. Schulz. A modular degree-of-interest specification for the visual analysis of large dynamic networks. *IEEE Transactions on Visualization and Computer Graphics*, 20(3):337–350, March 2014. doi: 10.1109/TVCG.2013.109

[2] P. A. Abrams. Consumer functional response and competition in consumer-resource systems. *Theoretical Population Biology*, 17(1):80–102, 1980.

[3] P. A. Abrams, R. D. Holt, and J. D. Roth. Apparent competition or apparent mutualism? shared predation when populations cycle. *Ecology*, 79(1):201–212, 1998.

[4] N. Andrienko and G. Andrienko. State transition graphs for semantic analysis of movement behaviours. *Information Visualization*, 17(1):41–65, 2018. doi: 10.1177/1473871617692841

[5] B. Bach, E. Pietriga, and J. Fekete. Graphdiaries: Animated transitions andtemporal navigation for dynamic networks. *IEEE Transactions on Visualization and Computer Graphics*, 20(5):740–754, 2014.

[6] F. Beck, M. Burch, S. Diehl, and D. Weiskopf. The state of the art in visualizing dynamic graphs. In *EuroVis*, 2014.

[7] E. Benincà, J. Huisman, R. Heerkloss, K. D. Jöhnk, P. Branco, E. H. Van Nes, M. Scheffer, and S. P. Ellner. Chaos in a long-term experiment with a plankton community. *Nature*, 451(7180):822, 2008.

[8] E. Benincà, K. D. Jöhnk, R. Heerkloss, and J. Huisman. Coupled predator–prey oscillations in a chaotic food web. *Ecology letters*, 12(12):1367–1378, 2009.

[9] J. Berlin. Semiology of graphics: Diagrams, networks, maps. *Trails. William J. Berg. Madison: U of Wisconsin P*, 1983.

[10] J. Blaas, C. Botha, E. Grundy, M. Jones, R. Laramee, and F. Post. Smooth graphs for visual exploration of higher-order state transitions. *IEEE Transactions on Visualization and Computer Graphics*, 15(6):969–976, 2009.

[11] M. Brehmer, M. Sedlmair, S. Ingram, and T. Munzner. Visualizing dimensionally-reduced data: Interviews with analysts and a characterization of task sequences. In *Proceedings of the Fifth Workshop on Beyond Time and Errors: Novel Evaluation Methods for Visualization*, pp. 1–8, 2014.

[12] M. Burch, B. Schmidt, and D. Weiskopf. A matrix-based visualization for exploring dynamic compound digraphs. In *2013 17th International Conference on Information Visualisation*, pp. 66–73. IEEE, 2013.

[13] C.-W. Chang, M. Ushio, and C.-h. Hsieh. Empirical dynamic modeling for beginners. *Ecological research*, 32(6):785–796, 2017.

[14] E. R. Deyle, M. Fogarty, C.-h. Hsieh, L. Kaufman, A. D. MacCall, S. B. Munch, C. T. Perretti, H. Ye, and G. Sugihara. Predicting climate effects on pacific sardine. *Proceedings of the National Academy of Sciences*, 110(16):6430–6435, 2013.

[15] E. R. Deyle, R. M. May, S. B. Munch, and G. Sugihara. Tracking and forecasting ecosystem interactions in real time. *Proceedings of the Royal Society B: Biological Sciences*, 283(1822):20152258, 2016. doi: 10.1098/rspb.2015.2258

[16] P. A. Dixon, M. J. Milicich, and G. Sugihara. Episodic fluctuations in larval supply. *Science*, 283(5407):1528–1530, 1999.

[17] T. Falkowski, J. Bartelheimer, and M. Spiliopoulou. Mining and visualizing the evolution of subgroups in social networks. In *Proceedings of the 2006 IEEE/WIC/ACM International Conference on Web Intelligence*, pp. 52–58. IEEE Computer Society, 2006.

[18] T. Fujiwara, O. Kwon, and K. Ma. Supporting analysis of dimensionality reduction results with contrastive learning. *IEEE Transactions on Visualization and Computer Graphics*, 26(1):45–55, 2020.

[19] C. Gratton and R. F. Denno. Seasonal shift from bottom-up to top-down impact in phytophagous insect populations. *Oecologia*, 134(4):487–495, 2003.

[20] S. Hadlak, H. Schumann, C. H. Cap, and T. Wollenberg. Supporting the visual analysis of dynamic networks by clustering associated temporal attributes. *IEEE Transactions on Visualization and Computer Graphics*, 19(12):2267–2276, Dec 2013. doi: 10.1109/TVCG.2013.198

[21] A. Hastings and T. Powell. Chaos in a three-species food chain. *Ecology*, 72(3):896–903, 1991.

[22] H. Hotelling. Analysis of a complex of statistical variables into principal components. *Journal of educational psychology*, 24(6):417, 1933.

[23] D. A. Keim. Information visualization and visual data mining. *IEEE Transactions on Visualization and Computer Graphics*, 8(1):1–8, Jan 2002. doi: 10.1109/2945.981847

[24] J. B. Kruskal. Multidimensional scaling by optimizing goodness of fit to a nonmetric hypothesis. *Psychometrika*, 29(1):1–27, 1964.

[25] M. Lima, S. K. M. Ernest, J. H. Brown, A. Belgrano, and N. C. Stenseth. Chihuahuan desert kangaroo rats: Nonlinear effects of population dynamics, competition, and rainfall. *Ecology*, 89(9):2594–2603, 2008. doi: 10.1890/07-1246.1

[26] M. Lima, N. C. Stenseth, and F. M. Jaksic. Food web structure and climate effects on the dynamics of small mammals and owls in semi-arid chile. *Ecology Letters*, 5(2):273–284, 2002. doi: 10.1046/j.1461-0248.2002.00312.x

[27] L. v. d. Maaten and G. Hinton. Visualizing data using t-sne. *Journal of machine learning research*, 9(Nov):2579–2605, 2008.

[28] M. C. Maher and R. D. Hernandez. Causemap: fast inference of causality from complex time series. *PeerJ*, 3:e824, 2015.

[29] K. Mizuno, H.-Y. Wu, S. Takahashi, and T. Igarashi. Optimizing stepwise animation in dynamic set diagrams. *Computer Graphics Forum*, 38(3):13–24, 2019. doi: 10.1111/cgf.13668

[30] H. Natsukawa and K. Koyamada. Visual analytics of brain effective connectivity using convergent cross mapping. In *SIGGRAPH Asia 2017 Symposium on Visualization*, SA '17, pp. 6:1–6:9. ACM, New York, NY, USA, 2017. doi: 10.1145/3139295.3139303

[31] L. G. Nonato and M. Aupetit. Multidimensional projection for visual analytics: Linking techniques with distortions, tasks, and layout enrichment. *IEEE Transactions on Visualization and Computer Graphics*, 25(8):2650–2673, 2019.

[32] K. Pearson. Liii. on lines and planes of closest fit to systems of points in space. *The London, Edinburgh, and Dublin Philosophical Magazine and Journal of Science*, 2(11):559–572, 1901.

[33] E. R. Pianka. On r- and k-selection. *The American Naturalist*, 104(940):592–597, 1970. doi: 10.1086/282697

[34] D. M. Post, M. E. Conners, and D. S. Goldberg. Prey preference by a top predator and the stability of linked food chains. *Ecology*, 81(1):8–14, 2000.

[35] A. J. Pretorius and J. J. Van Wijk. Visual analysis of multivariate state transition graphs. *IEEE Transactions on Visualization and Computer Graphics*, 12(5):685–692, Sep. 2006. doi: 10.1109/TVCG.2006.192

[36] R. C. Roberts, D. Rees, R. S. Laramee, P. Brookes, and G. A. Smith. RiverState: A Visual Metaphor Representing Millions of Time-Oriented State Transitions. In *Computer Graphics and Visual Computing (CGVC)*. The Eurographics Association, 2018. doi: 10.2312/cgvc.20181210

[37] S. T. Roweis and L. K. Saul. Nonlinear dimensionality reduction by locally linear embedding. *science*, 290(5500):2323–2326, 2000.

[38] B. Shneiderman. The eyes have it: A task by data type taxonomy for information visualizations. In *Proceedings 1996 IEEE symposium on visual languages*, pp. 336–343. IEEE, 1996.

[39] M. Steiger, J. Bernard, S. Mittelstädt, H. Lücke-Tieke, D. Keim, T. May, and J. Kohlhammer. Visual analysis of time-series similarities for anomaly detection in sensor networks. In *Computer graphics forum*, vol. 33, pp. 401–410. Wiley Online Library, 2014.

[40] G. Sugihara, W. Allan, D. Sobel, and K. D. Allan. Nonlinear control of heart rate variability in human infants. *Proceedings of the National Academy of Sciences*, 93(6):2608–2613, 1996. doi: 10.1073/pnas.93.6.2608

[41] G. Sugihara, B. T. Grenfell, R. M. May, and H. Tong. Nonlinear forecasting for the classification of natural time series. *Philosophical Transactions of the Royal Society of London. Series A: Physical and Engineering Sciences*, 348(1688):477–495, 1994. doi: 10.1098/rsta.1994.0106

[42] G. Sugihara, R. May, H. Ye, C.-h. Hsieh, E. Deyle, M. Fogarty, and S. Munch. Detecting causality in complex ecosystems. *science*, 338(6106):496–500, 2012.

[43] G. Sugihara and R. M. May. Nonlinear forecasting as a way of distinguishing chaos from measurement error in time series. *Nature*, 344(6268):734, 1990.

[44] SugiharaLab. redm. https://github.com/SugiharaLab/rEDM, 2018.

[45] SugiharaLab. pyedm. https://github.com/SugiharaLab/pyEDM, 2019.

[46] J. B. Tenenbaum, V. De Silva, and J. C. Langford. A global geometric framework for nonlinear dimensionality reduction. *science*, 290(5500):2319–2323, 2000.

[47] E. R. Tufte. *The visual display of quantitative information*, vol. 2. Graphics press Cheshire, CT, 2001.

[48] United Nations. *Transforming our world: the 2030 agenda for sustainable development.*, 2015.

[49] M. Ushio. Interaction capacity underpins community diversity. *bioRxiv*,

2020. doi: 10.1101/2020.04.08.032524

[50] M. Ushio, C.-h. Hsieh, R. Masuda, E. R. Deyle, H. Ye, C.-W. Chang, G. Sugihara, and M. Kondoh. Fluctuating interaction network and time-varying stability of a natural fish community. *Nature*, 554(7692):360, 2018.

[51] M. Ushio, Y. Osada, T. Kumagai, T. Kume, R. a. S. Pungga, T. Nakashizuka, T. Itioka, and S. Sakai. Dynamic and synergistic influences of air temperature and rainfall on general flowering in a bornean lowland tropical forest. *Ecological Research*, 35(1):17–29, 2020. doi: 10.1111/1440-1703.12057

[52] S. van den Elzen, D. Holten, J. Blaas, and J. J. van Wijk. Reducing snapshots to points: A visual analytics approach to dynamic network exploration. *IEEE Transactions on Visualization and Computer Graphics*, 22(1):1–10, Jan 2016. doi: 10.1109/TVCG.2015.2468078

[53] L. Van Der Maaten. Barnes-hut-sne. *arXiv preprint arXiv:1301.3342*, 2013.

[54] L. Van Der Maaten, E. Postma, and J. Van den Herik. Dimensionality reduction: a comparative review. *J Mach Learn Res*, 10(66-71):13, 2009.

[55] F. van Ham, H. van de Wetering, and J. J. van Wijk. Interactive visualization of state transition systems. *IEEE Transactions on Visualization and Computer Graphics*, 8(4):319–329, Oct. 2002. doi: 10.1109/TVCG.2002.1044518

[56] T. von Landesberger, S. Diel, S. Bremm, and D. W. Fellner. Visual analysis of contagion in networks. *Information Visualization*, 14(2):93–110, 2015.

[57] J. Wenskovitch, I. Crandell, N. Ramakrishnan, L. House, S. Leman, and C. North. Towards a systematic combination of dimension reduction and clustering in visual analytics. *IEEE Transactions on Visualization and Computer Graphics*, 24(1):131–141, 2018.

[58] H. Ye, E. R. Deyle, L. J. Gilarranz, and G. Sugihara. Distinguishing time-delayed causal interactions using convergent cross mapping. *Scientific reports*, 5:14750, 2015.